



HAL
open science

Characterization of the Algal Colonization of Mortar Surfaces Using Image Analysis

Juliette Hortemel, Sara Zaghoul, Alexandre Govin, Johan Debayle

► **To cite this version:**

Juliette Hortemel, Sara Zaghoul, Alexandre Govin, Johan Debayle. Characterization of the Algal Colonization of Mortar Surfaces Using Image Analysis. *Image Analysis & Stereology*, 2024, 43 (2), pp.159 - 166. 10.5566/ias.3165 . emse-04651900

HAL Id: emse-04651900

<https://hal-emse.ccsd.cnrs.fr/emse-04651900v1>

Submitted on 17 Jul 2024

HAL is a multi-disciplinary open access archive for the deposit and dissemination of scientific research documents, whether they are published or not. The documents may come from teaching and research institutions in France or abroad, or from public or private research centers.

L'archive ouverte pluridisciplinaire **HAL**, est destinée au dépôt et à la diffusion de documents scientifiques de niveau recherche, publiés ou non, émanant des établissements d'enseignement et de recherche français ou étrangers, des laboratoires publics ou privés.



Distributed under a Creative Commons Attribution 4.0 International License

CHARACTERIZATION OF THE ALGAL COLONIZATION OF MORTAR SURFACES USING IMAGE ANALYSIS

JULIETTE HORTEMEL, SARA ZAGHLOUL, ALEXANDRE GOVIN AND JOHAN DEBAYLE✉

MINES Saint Etienne, CNRS, UMR 5307 LGF, Centre SPIN, F - 42023 Saint-Etienne France
e-mail: hortemel.juliette@gmail.com, sarazaghoul.sz@gmail.com, govin@emse.fr, debayle@emse.fr
(Received February 22, 2024; revised June 4, 2024; accepted June 4, 2024)

ABSTRACT

This research work aims to characterize the algal colonization of mortar surfaces using image analysis. The resistance of mortars to the biofouling is studied by means of an accelerated lab-scale test. A suspension of green algae *Klebsormidium flaccidum*, was performed to periodically sprinkle the mortar surfaces and digital images were acquired thanks to a scanner. The colonization rate of the surface follows a sigmoid type curve as a function of time that can be modeled thanks to Avrami's model. It is described by a two-process mechanism: attachment and growth of algal stains. To identify the parameters of the algal colonization model, the images were segmented thanks to a random forest algorithm to obtain pixel information on the presence of algae. These processes were then represented with a morphological min-tree and information such as the number of new germs or their growth have been exploited to feed the Avrami's model. The results show a good agreement between the modeling and the experimental data.

Keywords: Avrami's model, component-trees, image analysis, image segmentation, random forest.

INTRODUCTION

The building facades are progressively and inevitably subjected to biological colonization inducing physical and aesthetical degradations of the construction. The involved microorganisms are bacteria, algae, cyanobacteria, fungi, lichens and even higher plants if no prevention is applied. The implantation of microorganisms depends on many factors such as climate, environment, light, relative humidity, roughness, porosity, chemical composition, surface pH... (Ortega-Calvo *et al.*, 1995). Several studies were devoted to the investigation of the influence of these parameters on biofouling, at laboratory scale as well as at real scale.

In the literature, some authors have attempted to model this phenomenon (Tran *et al.*, 2013). They showed that Avrami's germination-growth model was quite a good tool to express the temporal evolution of the colonization rates. Avrami's model is based on two processes: the nucleation, corresponding to the appearance of nuclei of a new phase and the growth representing the increase in the size of these nuclei with time. In this work, the colonization rate follows a sigmoid type curve as a function of time and the biofouling is initiated by the attachment of algae on the surface of samples creating many spots and considered as nuclei. As a consequence, the colonization can be modeled by Avrami's model.

The aim of this work is to characterize the colonization mechanism of materials by algae using

image analysis. Avrami's model parameter values are extracted using a morphological tree structure and used to model the algal colonization phenomenon. The main contributions concern the use of a tree structure to represent the image sequence (algal colonization at different times) and the corresponding characterization to feed the model.

The paper is organized as follows. The next section shows the experimental setup for image acquisition, the Avrami's model, the segmentation of images, the tree structure and the determination of the model parameters. Thereafter the experimental and simulated results are compared and discussed. A conclusion and some prospects close the paper.

MATERIALS AND METHODS

EXPERIMENTAL DATA

Samples were made up of a cement-based substrate covered by a render, composed of white Portland cement CEM I 52.5 N, calcareous filler, a thickener and water. The render was deposited thanks to a roughcast roller onto the surface of the substrates. After storage at $21 \pm 1^\circ\text{C}$ and $95 \pm 5\%$ of relative humidity for 10 days, the render was carbonated under pure CO_2 in order to decrease the surface pH to around 9, allowing the algal colonization. The size of the samples were $20 \times 8 \times 1 \text{ cm}$. The studied algal specie was *Klebsormidium flaccidum* because of its representativeness and its ease of cultivation.

The bio-receptivity of mortar was examined through a laboratory accelerated test. The experimental device consists in a $100 \times 50 \times 50$ cm closed glass chamber placed in a dark room. Samples were placed on a stainless steel support inclined at 45° . 50 L of sterilized culture medium with an initial algal concentration of 4 mg.L^{-1} was introduced. The suspension was sprinkled onto samples by means of pumps for 90 minutes every 12 hours. Light was provided by neon lamps with a photoperiod of 12 hours. In the presented test, 8 samples were placed into the chamber. This experimental approach is more detailed in (Tran *et al.*, 2012).

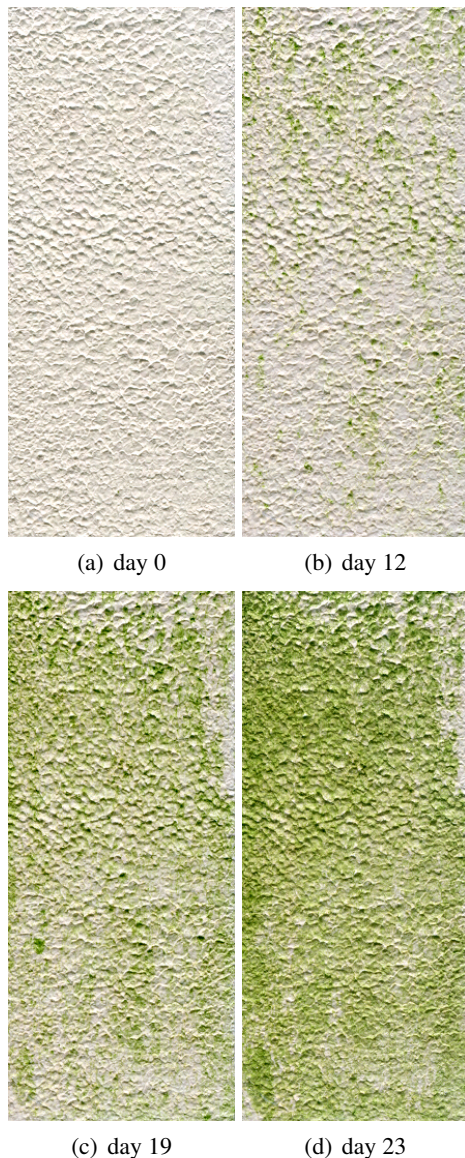


Fig. 1. Images of a mortar colonized by algae at different time.

To evaluate biofouling, the sample surface was daily digitized by means of an office scanner. The spatial resolution of the scanner is 600 dpi. Fig. 1

shows some images of one mortar sample colonized by algae, acquired at different times.

MODEL OF THE ALGAL COLONIZATION

The modeling of the algal colonization, using Avrami's model, is based on two main processes (Tran *et al.*, 2013): the attachment rate and the growth rate.

Attachment rate

The attachment rate was defined as the number of algal spots appearing on surface unit per time unit and was modeled thanks to a power law.

$$\frac{d\gamma}{dt}(t) = k_g(t - t_l)^q \quad (1)$$

where $\gamma(t)$ is the number of algal spots at time t per unit area ($\text{spots}/\mu\text{m}^2$). The constant q denotes the power of the germination law. k_g is the attachment specific rate constant ($\text{spots}/\mu\text{m}^2 \cdot \text{day}^{q+1}$). t_l corresponds to the latency time (day) and denotes the beginning of nucleation and thus colonization.

Growth rate

The growth was considered as two-dimensional and the hypotheses that the growth rate was identical for all algal spots and constant during time were applied. The surface area at time t covered by an algal spot appearing at time θ was expressed as follows:

$$S(t) = k_c^2 \cdot (t - \theta)^2 \quad (2)$$

where k_c corresponds to the specific growth rate constant ($\mu\text{m}/\text{day}$).

The final model

Finally, from Avrami's model, the colonization rate $X(t)$ at time t is calculated from the law of nucleation and growth as an exponential equation:

$$X(t) = 1 - \exp\left(-\frac{2k_g k_c^2 (t - t_l)^{q+3}}{(q+1)(q+2)(q+3)}\right) \quad (3)$$

In this equation, k_c , k_g , q , t_l are constants defined in the previous equations 1 and 2.

In this study, t_l is considered to be the time at which the algae cover 0.1 percent of the surface and q is assumed equal to 1, i.e. one can extrapolate the law of speed of germination to a line, relating to the germination of uniform probability, which means that there is an identical probability regardless of the location of the germ. More details can be found in (Tran *et al.*, 2013)

The objective of this work is then to estimate these two specific rate constants (i.e. k_c and k_g) by using

image analysis, so as to get a simulated colonization rate $\hat{X}(t)$ by using Equation 3. It will be compared to the experimental colonization rate $X(t)$ computed on each image by simply calculating the density of the pixels classified as algae.

To estimate k_c and k_g , the necessary characteristics of the colonization are the number of algal spots appearing on surface unit per time unit (attachment rate) and the surface area at time $t+x$ covered by an algal spot appearing at time t (growth rate). To access those parameter values, images are required to be firstly segmented in order to be thereafter quantified for extracting the attachment of algae.

IMAGE SEGMENTATION

The objective of this segmentation is to generalize the detection of the biocolonization of mortars in the case of in-situ tests where different microorganisms and thus different colors can be observed on the surface of samples. Given the variability of the images (colors of algae, tints, shadows ...), the usual segmentation techniques such as thresholding are not suitable.

In the literature, image segmentation can be divided in two classes, those based on traditional techniques (such as (Gutman *et al.*, 2024)) and those based on machine learning techniques (such as (Minaee, 2021; Kirillov *et al.*, 2023)). In order to take into account images of various mortars colonized by the algae in different conditions, a machine learning-based segmentation method based on pixel supervised classification (Posada-Gómez *et al.*, 2011) was investigated in this paper. The desired binary classifier has two possible outputs : pixel covered by algae or not. The advantage of using such an automatic generic segmentation is its ability to adapt to several mortars presenting various specific properties in terms of composition, rugosity, roughness, color, lightness, ... (using a suitable training set).

Building a dataset

Images from a unique sequence corresponding to a specific experiment (with mortar composed of white Ordinary Portland Cement, roughness $Ra = 150 \mu\text{m}$, initial surface $pH = 9.1$) and composed of 15 images (as shown in the experimental data) are segmented by combining thresholding operators (Posada-Gómez *et al.*, 2011) performed on the color components. The parameters were empirically tuned by an expert so as get a suitable segmentation from a visual point of view. These segmented images are then considered as the ground truth. One can note that there does not exist an objective criterion to define this ground truth. Different samples are thereafter selected to build the training

dataset. More precisely, 7 regions of size 500×700 pixels have been randomly selected and cropped from the image sequence. Thereafter 3000 pixels classified as algae and 3000 pixels classified as background have been randomly selected to build the dataset.

Pixel features

For each image, the pixels are described in the (L, a, b) color space, since the classical (R, G, B) color space does not give significant contrast to separate the algae and the background.

The used features are based on texture and morphological characteristics. Local Binary Patterns (LBP) (Ojala *et al.*, 2002) are used for the texture description and operators from mathematical morphology (erosion and dilation) are used for the morphological description (Soille, 2003) .

For both texture and morphological pixel description, the radius varies between the following values: 2, 4, 6, 8, in order to work on different neighborhood scales. In this way, four different values for each pixel are obtained as each carries the information depending on different neighboring pixels. This process is applied to all three channels of the image and a total of 36 features for each pixel is then obtained.

Classification models

Different classifiers' performances are compared. The selected classifiers are: Multi-Layer-Perceptron (MLP), Random Forest (RF), Support Vector Machine (SVM) and Vote. The later corresponds to the most frequently chosen class considering all previous classifiers after a bagging of the data. The results will be shown on the next section.

IMAGE SEQUENCE ANALYSIS USING COMPONENT-TREES

Once the images are segmented and pixels are annotated with labels (algae or not), the over-time coverage of the surface by algae is accessed. The processes at stake are germ spots appearing, growing and merging together. To apply Avrami's model, the necessary parameters are the number of algal spots appearing on surface unit per time unit (attachment rate) and the surface area at time $t + x$ covered by an algal spot appearing at time t (growth rate).

The use of a tree structure (Bosilj *et al.*, 2018) facilitates the access to those parameters. The leaves of the tree correspond to the germs being born, the subbranches to growing spots and the nodes that have multiple children to the merging of spots. This

representation will enable to extract the quantitative information as inputs for the model description. The desired tree structure is shown in Fig. 2 on a toy example. The images on the top correspond to the evolution of the mortar surface colonized by algae spots (shown in white, background is black) at different times. The numbers both corresponds to the connected components of the binary images and the nodes into the hierarchical tree. The blue nodes corresponds to germ nucleation, the red to germ growth and the pink ones as germ fusion. All the required information for the Avrami's model parameters is then contained in such a hierarchical tree.

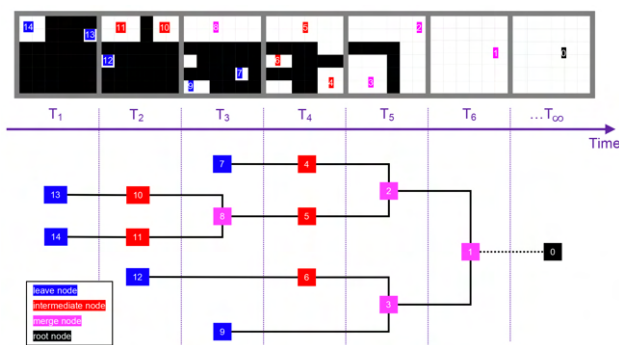


Fig. 2. *Desired tree structure on a toy example. A sequence of images at different times is shown at the top (the white components correspond to the algae spots). At the bottom, the corresponding tree of components is illustrated. It contains all the required information (nucleation, growth and merge of algae spots).*

The most widespread forms of hierarchical tree structures are detailed in Bosilj *et al.* (2018). Component trees are found in many applications : classification, image filtering, segmentation, registration, compression and morphological operators, for instance algebraic openings/closings and levellings. (Berger *et al.*, 2007). Many theoretical publications describe the efficient implementation of some of these trees (Géraud *et al.*, 2013; Perret *et al.*, 2010). These tree structures are used in many applications : astronomy (Perret *et al.*, 2010), biology (Oliveira *et al.*, 2018) and many others.

To build the desired tree for the proposed study in this paper, the selected structure is a morphological Min-tree of components, as first introduced in (Salembier *et al.*, 1998). The Min-tree is an inclusion tree representing the dark structures in an image I , based on lower level sets with the leaves corresponding to the local image minima. A connected component of the level set L_k missing from the level set L_{k-1} makes a

new node n_k with its surrounding spatial region $R(n_k)$ which becomes either :

- A parent node to all previous nodes at lower levels which are included in the region of the new node: $R(n_{k'}) \subset R(n_k), k' < k$.
- A leaf node if it does not include the regions of any previous nodes.

At the highest gray level, there is only one connected component covering the whole image and it forms the root of the tree. The hierarchy corresponds to distinct connected components of the lower level sets: $H_{min} = \{CC(L_k) | k \leq l_{Max}\}$. The local minima of the dual image $-I$ correspond to the local maxima of the original. Thus, considering the upper level sets of I or the lower level sets of the dual $-I$, one obtain the dual Max-tree hierarchy. The Min-tree is adapted for manipulation of dark image structures, and the Max-tree, based on higher level sets with the leaves corresponding to the local image maxima, for the bright ones (Bosilj *et al.*, 2018).

The structure of Min and Max trees is shown in Fig. 3, extracted from Bosilj *et al.* (2018).

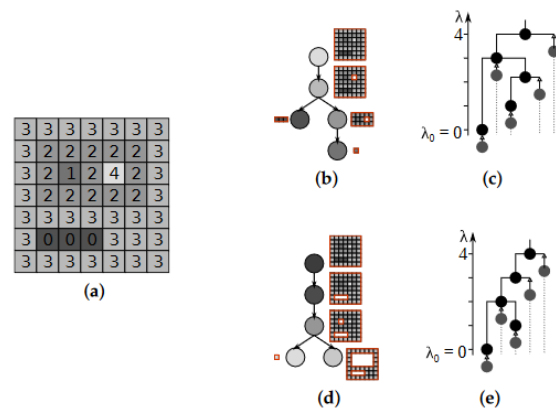


Fig. 3. (a) *The original image; (b) corresponding Min-tree; (c) the dendrogram; and (d,e) Max-tree and its dendrogram. Corresponding spatial regions are shown next to the nodes. Extracted from Bosilj et al. (2018)*

To use the presented data as a Min-tree, the temporality of the evolution will be represented in the following way : a superimposition of the binary algae segmented images is used, representing the older apparition of algae darker in gray-level, with a grey-value corresponding to the time at which they appeared. This leads to nested structures as we consider no algae detachment. A "final" image is constructed with only zeros so that it corresponds to the root of the tree.

DETERMINATION OF k_g AND k_c

The identification of the parameters values of k_g and k_c from the Avrami's model is then possible by extracting information from the tree structure.

Determination of k_g

To extract the required model parameters, only the data up to the day 16 is considered. After 16 days, it is difficult to perfectly identify the new spots, as the colonization rate exceeds 50% leading to a significant overlap between the new spots and the existing algal deposit. This results in poor quantification of the number of new spots. Further data contain algae detachment which does not fit within the scope of this study. The extraction of the number of new germs per remaining surface over time from the tree is performed and the time at which they appeared is accessed sorting them by gray-level as explained earlier. To obtain the value of k_g , the number of new germs per remaining surface as a function of time is extracted considering the leaves of the tree. This function is then derived with respect to time and plotted as a function of $t - t_l$ (we assume $q = 1$). A linear regression is performed and the slope is extracted as k_g .

Determination of k_c

The surface covered by growing germs over time is extracted. The growth of only non-merging germs is considered given that considering the growth of merging would not be accurate.

These alone germs are the subbranches of the tree. To extract the subbranches, all leave nodes and merging nodes (nodes that have multiple children) are considered. We then consider each of this nodes and proceed to loop alongside the subbranch and extract the unique parent of the considered node until the parent is not unique, e.g. when a merging occurs.

For every germ, its growth is followed, the surface $S(t)$ is plotted in pixels according to the square of $(t - \theta)$. The intercept is forced to zero as a linear relation is seek.

All the values obtained for each subbranch are averaged to obtain the final k_c .

More computational details for the determination of the values k_g and k_c can be found in Tran *et al.* (2013).

RESULTS

CLASSIFICATION RESULTS FOR IMAGE SEGMENTATION

A 5-fold cross validation is performed to ensure generalization of the models. The results from the different classifiers are presented in table 1 using different performance metrics. Best results are highlighted in bold font.

Table 1. *Performance evaluation of different classifiers.*

	MLP	RF	SVM	Vote
Accuracy	95.6%	99.3%	98%	98.5%
F1 score	94.4%	99.0%	97.8%	98.6%
Jacquard index	89.5%	98.1%	95.8%	97.2%
Matthews CC	90.2%	98.1%	95.6%	97.3%

For the RF classifier, 500 trees and a maximum depth of 16 have been used. Regarding the MLP classifier, the hyperparameters are: 10 layers and 10 neurons in each layer, the stochastic gradient-based optimizer and a maximum of 1000 iterations. For the SVM classifier, a linear kernel has been used.

The Random Forest algorithm yields better results and takes reasonable calculation time. The final segmentation is therefore performed using this RF classifier.

EXTRACTION OF AVRAMI PARAMETERS AND MODELING

Based on the methodology detailed earlier, the following values were obtained : $t_l = 4.63$ days, $k_g = 2.55 \cdot 10^{-8}$ spots per squared day t^2 per μm^2 and $k_c = 178.1 \mu m$ per day. These parameters lead to the simulation shown in Fig. 4.

DISCUSSION

The results show a quite good agreement between the modeling and the experimental data. However, there are differences observed between the ground truth and the simulation with the empirical values, which could come from the fact that the few drop-off of algae are not taken into account since it is considered that each image is included in the next one. In addition, it was assumed in this paper $q = 1$ but a power law different than one could be considered.

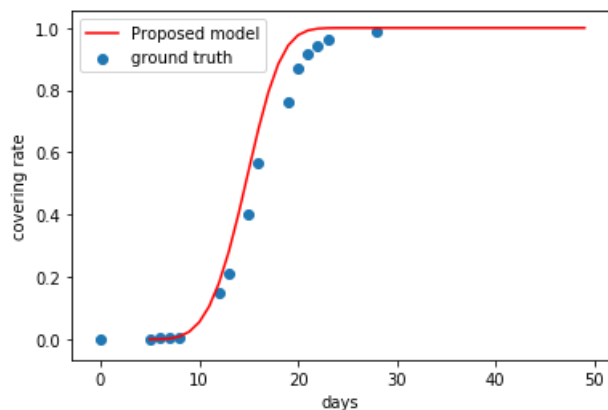


Fig. 4. Simulation of the covering rate with the proposed model compared to the ground truth corresponding to the experimental data.

CONCLUSION AND PROSPECTS

The aim of this study was to introduce a reproducible method to extract Avrami's parameters from a case of colonization of mortar surface by algae. Thanks to image acquisition and analysis, the model parameter values have been extracted. The surface colonization all along the time has been evaluated between the model and its direct characterization from images, showing a quite well agreement. The results could be improved by taking into account the algae detachment by using a topological tracking of connected components in image sequences (Gonzalez-Diaz *et al.*, 2018), but it could be difficult to experimentally quantify this phenomenon. Also, the acquisition setup could be improved by using other acquisition systems than the scanner.

The strength of the proposed method in relation to the studied application is the use of a component tree applied to an image sequence. Indeed, it gives directly access to the required information (nucleation, growth and fusion of the algae spots) leading to an easy characterization. The main limitation is the lack of a ground truth for the image segmentation step, although an expert can provide an estimate based on qualitative considerations.

Finally, if the proposed generic method is used on different scenario, the influence of several parameters such as climate, environment, light, relative humidity, roughness, porosity, chemical composition or surface pH could be investigated.

REFERENCES

Berger C, Géraud T, Levillain R, Widynski N, Baillard A, Bertin E (2007). Effective component

tree computation with application to pattern recognition in astronomical imaging. In: IEEE C Image Proc.

Bosilj P, Kijak E, Lefèvre S (2018). Partition and inclusion hierarchies of images: A comprehensive survey. *J Imaging* 4:1–33.

Gonzalez-Diaz R, Jimenez M, Medrano B (2018). Topological tracking of connected components in image sequences. *J Comput Syst Sci* 95:134–42.

Gutman Z, Vij R, Najman L, Lindenbaum M (2024). Assessing hierarchies by their consistent segmentations. *J Math Imaging Vis* 66:314–34.

Géraud T, Carlinet E, Crozet S, Najman L (2013). A quasi-linear algorithm to compute the tree of shapes of nd images. In: *Int Symp Math Morph.*

Kirillov L, Mintun E, Ravi N, Mao H, Rolland C, Gustafson L, Xiao T, Whitehead S, Berg A, Lo WY, Dollar P, Girschick RB (2023). Segment anything. *IEEEI Conf Comp Vis* :4015–26.

Minaee S (2021). Image segmentation using deep learning: A survey. *J Comput Syst Sci* 44:3523–42.

Ojala T, Pietikäinen M, Mäenpää T (2002). Multiresolution gray-scale and rotation invariant texture classification with local binary patterns. *IEEE Trans Pattern Anal Mach Intell* 24:971–87.

Oliveira LM, Ye Z, Katz A, Alimova A, Wei H, Herman GT, Gottlieb P (2018). Component tree analysis of cystovirus phi6 nucleocapsid cryo-em single particle reconstructions. *Plos one* 13:e0188858.

Ortega-Calvo JJ, Ariño X, Hernandez-Marine M, Saiz-Jimenez C (1995). Factors affecting the weathering and colonization of monuments by phototrophic microorganisms. *Sci Total Environ* 167:329–41.

Perret B, Lefèvre S, Collet C, Slezak E (2010). Connected component trees for multivariate image processing and applications in astronomy. In: *Int C Patt Recog.*

Posada-Gómez R, Sandoval-González OO, Sibaja AM, Portillo-Rodríguez O, Alor-Hernández G (2011). Practical Applications and Solutions Using LabVIEW Software, chap. Digital image processing using LabVIEW. InTech, 297–316.

Salembier P, Oliveras A, Garrido L (1998). Anti-extensive connected operators for image and sequence processing. *IEEE Image Proc* 7:555–70.

Soille P (2003). *Morphological image analysis : principles and applications*, 2nd edition. Springer Berlin.

Tran TH, A. G, Guyonnet R, Grosseau P, Lors C, Garcia-Diaz E, Ruot B (2012). Influence of the

intrinsic characteristics of mortars on biofouling by klebsormidium flaccidum. *Int Biodeter Biodegr* 70:31–9.

Tran TH, Govin A, Guyonnet R, Grosseau P, Lors C,

Damidot D, Ruot B (2013). Avrami's law based kinetic modeling of colonization of mortar surface by alga klebsormidium flaccidum. *Int Biodeter Biodegr* 1:73–80.